Research Square

Preprints are preliminary reports that have not undergone peer review.
They should not be considered conclusive, used to inform clinical practice,
or referenced by the media as validated information.

A null adult postmortem-brain test of a locked 468-gene panel in autism spectrum disorder, with published maternal-axis architecture as context

Mark E. McCaulley

mark@siriusneuroscience.com

Sirius Neuroscience, LLC https://orcid.org/0000-0003-2059-622X

Research Article

Keywords: autism spectrum disorder, transcriptomic meta-analysis, placenta, maternal–fetal interface, retinoic acid, gene–environment interaction

Posted Date: November 3rd, 2026

DOI: https://doi.org/10.21203/rs.3.rs-11553062/v1

License: This work is licensed under a Creative Commons Attribution 4.0 International License. Read Full License

Additional Declarations: The authors declare potential competing interests as follows: The author is the sole inventor on a filed patent application relating to panel-based research scoring methods that use the locked 468-gene list. MFS, mGVI, and ASD-IDRS in this paper are unvalidated and were not computed on empirical maternal samples. The application did not determine gene membership, the high-confidence rule, or the reported results. The author declares no other competing interests.

Abstract

Autism spectrum disorder (ASD) was examined in four primary adult postmortem-brain GEO cohorts (GSE102741, GSE28521, GSE269105, GSE64018) using a frozen 468-gene redox, metal, xenobiotic, and barrier panel. Inverse-variance random-effects meta-analysis (DerSimonian–Laird) produced 392 analyzable genes, one at Benjamini–Hochberg FDR < 0.05 (MAFK, lower in ASD), and no high-confidence genes (FDR < 0.05, measured in ≥ 3 cohorts, direction-concordant in ≥ 70% of cohorts, and nominally significant in ≥ 2 cohorts). Iron/redox–NRF2 genes that are higher in the neurodegenerative companions of this series were near zero and heterogeneous here (HMOX1 + 0.10, I^2 94%). Maternal whole blood (GSE148450) and umbilical cord blood (GSE123302) were also null at FDR < 0.05. Across 14 supporting developmental-model and postmortem datasets, per-dataset panel dysregulation tracked the breadth of the engineered lesion (broad regulatory or metabolic lesions 16–47% of panel genes; synaptic-scaffold models ≤ 7%) rather than the ASD label. Because adult brain samples a late, compensated tissue, I interpret the adult-brain null as constraining adult-brain transcriptional scarring, not the maternal–fetal interface. In first- versus third-trimester placenta (GSE247382; no ASD label), 459 of the 468 panel genes were measured and 320 expressed; placental polarity is descriptive context, not an ASD contrast. Conjugation and metal-handling genes were higher in the first trimester, barrier and steroid genes at term, and core NRF2-axis genes changed little. Published placental ASD evidence (a CYP2E1 methylation region in MARBLES; a 111-gene expression association in ELGAN) is cited, not re-analyzed. A compiled inventory of published detoxification-gene associations (MTHFR, CBS, PON1, GSTM1, GSTT1, GSTP1, ALDH2) was checked against the primary records for whose genotype was measured and which outcome was reported; only two entries are maternal-genotype ASD findings, both from one CHARGE analysis and both conditional on absent periconceptional prenatal vitamin use (maternal MTHFR 677 TT, OR 4.5, 95% CI 1.4–14.6; maternal CBS rs234715 GT + TT, OR 2.6, 95% CI 1.2–5.4), and the research formula mGVI is defined on those two. The remaining entries are child genotypes, non-ASD outcomes, interaction terms, or unsupported, and are retained as context only. mGVI, ASD-IDRS, and MFS were not computed on a maternal cohort, and none is a clinical tool. No proband detoxification-related variant in the assembled inventory reaches OR ≥ 1.5 in the GWAS summaries used. This paper is a disease-restricted companion to the methods-and-panel manuscript of this series (11).

Introduction

Autism spectrum disorder (ASD) affects approximately one in 31 children in the United States (2) and imposes one of the largest lifetime economic burdens of any developmental condition (1, 3). Its genetic architecture is dominated by rare de novo and inherited variants of large effect — including CHD8, SHANK3, SCN2A, and SYNGAP1, together with recurrent copy-number variants — which collectively account for roughly 25–35% of cases (4, 6, 7, 8, 9). Common-variant genome-wide association studies, by contrast, have identified no detoxification-pathway variant in the affected child (the proband) reaching an odds ratio of 1.5 or greater (10). That is a structural difference from the four neurodegenerative diseases analyzed in this series, in each of which proband detoxification variants of larger published effect exist (11, 12, 26, 27).

An adult-brain transcriptomic null would not exclude developmental, maternal, genetic, environmental, or cell-context-specific mechanisms. One testable hypothesis is that selected maternal-genome and gestational-window factors contribute to offspring risk during gestation weeks 4–28, when the fetus depends on maternal and placental detoxification capacity to buffer xenobiotic, oxidative, and one-carbon-metabolic stress (13, 24, 32).

Under this hypothesis a mother's inherited detoxification genotype, together with the fetal genotype expressed in the placenta, sets the capacity of the maternal–fetal interface, and its failure, particularly under environmental co-exposure, raises offspring ASD risk.

Published literature organizes candidate detoxification contributions into four axes, each framed around a gene–environment interaction, although the maternal-genotype ASD evidence within them is thinner than the framing suggests (Table 8). First, the one-carbon/folate axis, which carries the only maternal-genotype ASD findings in the inventory: in CHARGE, maternal MTHFR 677 TT and maternal CBS rs234715 GT + TT were associated with offspring ASD among mothers reporting no periconceptional prenatal vitamin use (OR 4.5, 95% CI 1.4–14.6, and OR 2.6, 95% CI 1.2–5.4) (31). Periconceptional folic acid intake of at least 600 µg/day was associated with lower offspring ASD odds in the same cohort programme (aOR 0.62, 95% CI 0.42–0.92; P for trend 0.001), most strongly in mothers and children carrying MTHFR 677 C > T variants (29), with an independent cohort of more than 85,000 mothers showing a 39% reduction (41) and lower recurrence in younger siblings (42). This is the most-replicated preventive association in ASD epidemiology. Reported MTHFR C677T associations in the child, by contrast, are child-genotype findings without a maternal subgroup (28, 30), and the commonly cited MTR and MTRR entries are not supported by the records to which they have been attributed (31, 39). Second, the paraoxonase/organophosphate axis: PON1 Q192R and − 108C > T have been studied as modifiers of prenatal organophosphate exposure, but in cohorts whose outcomes were cognitive and psychomotor measures rather than ASD (15, 16, 17, 40). Third, the glutathione S-transferase axis: GSTM1 and GSTT1 null genotypes are associated with ASD in the child (34), and GST genotypes modify heavy-metal associations (35, 36, 37); maternal-genotype ASD estimates are not available for this axis. Fourth, the aldehyde-detoxification axis: maternal alcohol consumption in pregnancy is associated with developmental delay, with ALDH2 genotype distinguishing which domains are affected, in a cohort whose outcome was a developmental screen rather than ASD (38).

To test whether these axes leave a transcriptional footprint, I applied the pre-specified 468-gene detoxification panel used across the companion diseases (11) to a locked four-cohort meta-analysis of adult postmortem brain and, descriptively, to 14 ASD transcriptomic datasets spanning developing-brain models (iPSC-derived neurons, neural progenitors, organoids, and defined genetic and exposure models) and adult postmortem brain. The adult-brain meta-analysis is essentially null, in contrast to the convergent adult-brain dysregulation seen in the neurodegenerative companions (11). I interpret that null as the absence of a reproducible adult-brain panel signature in the sampled cohorts. It is compatible with a developmental or maternal-window process that would not leave an ongoing adult-brain footprint; it does not prove such a process. CYP26 findings in developing-brain models are model- and stage-dependent and are absent from adult brain. The elevated later-life risk of Parkinson disease and early-onset dementia reported in autistic individuals (45, 46) is considered in the Discussion.

mGVI, ASD-IDRS, and MFS are described only as uncalibrated research formulae. They are not pre-conception metrics, diagnostic tools, or intervention selectors, and no value was computed on real maternal samples in this work.

Methods

Panel

The 468-gene panel is the frozen canonical panel of this series (v468; freeze 5 July 2026, analysis locked 6 July 2026), curated on mechanistic and pharmacogenomic grounds and not by feature selection within any ASD

dataset (11). Official tiers are CORE redox/metal/xenobiotic/barrier (394 genes), CORE cGAS–STING (12), CORE ferroptosis/iron/NRF2 (10), SENSITIVITY (40), and the placental/sex-steroid module (12; labelled 'ASD-maternal module' in the frozen panel file; that file label is not evidence the tier was selected on ASD data; not an inference set). For display the same 468 symbols are grouped into five functional hubs: Hub 1, xenobiotic and morphogen metabolism (230 genes); Hub 2, heavy-metal homeostasis (49); Hub 3, neuro-vascular integrity (40); Hub 4, antioxidant defense and redox homeostasis (92); Hub 5, transcriptional regulation (57). Hubs are an organizing device, not a second panel and not a pathway-enrichment test. The panel, excluded-symbol list, and methods are deposited at https://doi.org/10.5281/zenodo.22178094.

Locked adult postmortem-brain cohorts

Cohort assembly followed a documented, PRISMA-style provenance workflow (search → screen → de-duplicate by donor source → include), not a registered systematic review. A GEO DataSets search for human ASD expression studies (run 27 June 2026) returned approximately 727 records, which were screened to human ASD-versus-control postmortem brain with measurable bulk gene-level expression and then de-duplicated by donor source. Idiopathic ASD postmortem brain re-uses a small shared donor pool (Autism Tissue Program / Autism BrainNet and the NICHD/University of Maryland brain bank), so at most one accession per donor source was retained. Four independent cohorts form the locked meta-analysis (Table 1; donor provenance in Supplementary Table S2). GSE30573 (the RNA-seq component of Voineagu et al., ref. 20) was excluded for donor overlap with GSE28521.

Table 1
Locked adult postmortem-brain cohorts.

Accession	Tissue	Platform	n (ASD / control)	Donor source	Contrast statistics
GSE102741	Dorsolateral prefrontal cortex	Bulk RiboZero RNA-seq	13 / 39	Lieber Institute (LIBD); independent of ATP/Voineagu	DESeq2 (lfcSE)
GSE28521	Cerebellum (cerebellar arrays only; one array per donor)	Illumina HumanRef-8 v3 microarray (GPL6883)	10 / 11	ATP / Autism BrainNet (Voineagu et al. 2011)	|logFC / t|
GSE269105	Cerebellum	Bulk RNA-seq	3 / 2 (matched subset of 13)	Independent cerebellar cohort	DESeq2 (lfcSE)
GSE64018	Temporal cortex (BA41/42/22)	Bulk RNA-seq; raw counts	12 / 12	Gupta et al. 2014	PyDESeq2 on deposited counts (lfcSE)

ATP, Autism Tissue Program; LIBD, Lieber Institute for Brain Development.

Meta-analysis and high-confidence rule

The primary inferential result is a four-cohort inverse-variance random-effects meta-analysis (DerSimonian–Laird; ref. 53) of ASD-versus-control contrasts, pooled on the log2 fold-change scale. Per-gene standard errors were DESeq2 lfcSE for RNA-seq cohorts (55, 56) and |logFC / t| for the microarray cohort. For GSE28521, the cerebellar arrays (10 autism, 11 control; one array per donor) were used, and where a gene had more than one probe the probe with the lowest p value was retained (34 of 216 panel genes had more than one probe). Both choices were confirmed by re-deriving the GSE28521 contrast from the series matrix and checking it against the locked per-gene values: the cerebellar contrast was consistent with the locked direction and significance counts for all but one borderline gene (GSTZ1, p = 0.047), whereas frontal cortex, temporal cortex, and any pooling of regions or donors left 28–53 inconsistencies, and averaging probes added two. The earlier version of this paper described GSE28521 as cortex; that description was incorrect and is corrected here. Genes measured in at least two cohorts were meta-analyzed. Multiple-testing control used Benjamini–Hochberg FDR across the meta-analyzed panel genes (54). A gene is high-confidence when FDR < 0.05, it is measured in ≥ 3 of the four cohorts, direction is concordant in ≥ 70% of contributing cohorts, and it is nominally significant ($p < 0.05$) in ≥ 2 cohorts; for that criterion, cohort-level p values were computed from the normal approximation, $2\Phi(-|\text{logFC} / \text{SE}|)$. The rule is locked across the series (11) and is not relaxed here. In the Parkinson companion, lowest-p probe selection and the normal-approximation cohort p value were shown to inflate cohort-level evidence (27). Both can only add FDR-significant or high-confidence calls; neither can produce a null, so the ASD result is conservative with respect to them. Values are those of the locked workbook (CONSOLIDATED_468_FINAL_7.6.26.xlsx; per-gene tables at https://doi.org/10.5281/zenodo.22181129). Forest-plot confidence intervals in Fig. 1 were computed as pooled estimate ± 1.96 × SE, with SE recovered as |pooled| / z(p) because the deposited per-gene file does not carry standard errors.

Supporting per-dataset contrasts

I assembled 30 unique RNA-seq comparisons from 18 GEO accessions (Supplementary Table S1). After excluding two wild-type differentiation time-courses (GSE103715, GSE178896), one donor-overlapping cohort (GSE30573), and one NHIP-study brain dataset not used in the primary tier (GSE178205, 22q13.33/NHIP), 14 datasets form the per-dataset tier (one 468-panel contrast per accession; Table 4): 12 developing-brain datasets and two adult postmortem-brain datasets (GSE64018, GSE102741). One accession (GSE173687) was deleted by GEO staff on 20 September 2021 and is excluded. For each dataset the panel was applied to author-deposited DESeq2 top tables obtained through GEO2R (52) or, for GSE64018 (21), to deposited raw counts (GSE64018_countlevel_12asd_12ctl.txt) analyzed with PyDESeq2 (56) (12 ASD, 12 control); Ensembl identifiers were mapped to HGNC symbols with a curated table covering all 468 panel genes. Multiple GEO2R output files for one accession were de-duplicated by gene-set fingerprint. For the KDM2A, PTEN, valproate, and ASD-organoid contrasts, statistics were recomputed from NCBI-deposited raw counts with DESeq2 (55). The per-dataset significance threshold was Benjamini–Hochberg adjusted $P < 0.05$, with correction across all genes tested in that dataset (as reported by GEO2R and DESeq2), and $|\log2FC| \geq 0.5$. The Detoxification Dysregulation Index (DDI) is the percentage of panel genes (panel basis, ÷ 468) or measurable panel genes (measurable basis) reaching that threshold. DDI values are descriptive; they are not pooled and are not used to declare enrichment. Cross-dataset directional concordance is the fraction of comparisons, among those in which a gene reaches significance, in which it moves in the dominant direction. A 64-comparison GEO2R screen (covariate-unadjusted limma; ref. 57) was used only for hypothesis generation.

Cross-platform check

GSE28521 (Voineagu et al., ref. 20; Illumina HumanRef-8 v3, GPL6883; frontal cortex 16/16, temporal cortex 13/13, cerebellum 10/11) was analyzed within each region by independent-samples t-test with Benjamini–Hochberg correction; probe-to-symbol mapping used the WGCNA supplementary table of Voineagu et al., identifying 126 panel-gene probes. Uncorrected p values are shown for direction only (Supplementary Table S3).

Gestational-compartment datasets

Maternal peripheral blood from pregnancies later resulting in ASD or typical development (GSE148450, MARBLES; Zhu et al. (59): 300 samples across the three trimesters from pregnancies with ASD, non-typical, and typically developing outcomes) and umbilical cord blood (GSE123302, MARBLES and EARLI; Mordaunt et al. (58): Affymetrix Human Gene 2.0, 59 ASD and 120 typically developing across the two cohorts, with surrogate-variable adjustment in the original analysis) were screened on the panel with Benjamini–Hochberg correction within the panel. For maternal blood, GSE148450 as deposited contains 214 samples (56 ASD, 55 non-typical development, 103 typically developing outcomes). ASD (n = 56) was compared with typically developing (n = 103) outcomes in GEO2R (limma; default settings; no covariate adjustment) (52, 57); the 55 non-typical-development samples were excluded. The full table was restricted to panel genes and Benjamini–Hochberg correction was applied within the panel. GEO2R treats each sample as independent; whether any mother contributed samples from more than one trimester could not be determined from the deposit, and any such repetition would inflate, not reduce, apparent significance.

Placental ontogeny (descriptive; no ASD label)

To ask whether panel genes are expressed at the maternal–fetal interface, and in which gestational window, I used the first- versus third-trimester placenta RNA-seq atlas of Gonzalez et al. (49) (GSE247382; 124 first-trimester chorionic villus samples and 43 term placentas as deposited). NCBI-generated gene-level raw counts and TPM (GRCh38.p13) were available for 155 samples (113 first trimester, 42 term). Differential expression, term versus first trimester, was computed with PyDESeq2 (56) using the design ~ fetal sex + trimester, matching the authors' sex-adjusted model; genes with fewer than 10 total counts were removed, and 18 pregnancies sampled in both trimesters were treated as independent, as in the original analysis. The exact 468 locked symbols (11) were scored for mean TPM in each window and assigned to a window when $|\log_2 \text{fold-change}| \geq 0.5$ and Benjamini–Hochberg adjusted $p < 0.05$ (genome-wide). Per-gene values are in Supplementary Table S4. The series carries no ASD label; this is ontogeny, not an outcome contrast, and it is reported in the Discussion as context.

Maternal-axis literature inventory and research formulae

Published detoxification-gene associations were compiled into a literature inventory (Table 8). Each candidate entry was checked against the primary record to establish three things: whose genotype was measured (the mother's or the child's), what outcome was reported (ASD, another neurodevelopmental outcome, or clinical severity within cases), and whether the published estimate is a main effect or an interaction term. Entries qualify for the maternal genetic vulnerability index only if the genotype is maternal and the reported outcome is ASD in the offspring. Two entries qualify, both from the CHARGE analysis of Schmidt et al. (31) and both conditional on

absent periconceptional prenatal vitamin use: maternal MTHFR 677 TT (OR 4.5, 95% CI 1.4–14.6) and maternal CBS rs234715 GT + TT (OR 2.6, 95% CI 1.2–5.4). The index is therefore mGVI = Σ $\ln(OR_i)$ over those two variants. Cumulative OR = e^mGVI, and ASD-IDRS = mGVI + DDI/10, with DDI a percent (0–100). The additive form gives a nonzero score to an environmental-only profile (mGVI = 0, DDI > 0), where a multiplicative form would give zero. MFS is the individual-level, direction-aware Maternal Filter Score defined in the framework manuscript. An earlier version of this paper defined mGVI over seven primary variants spanning four axes; the source check reported in Table 8 found that five of those seven rested on child genotypes, non-ASD outcomes, or misattributed estimates, so that definition is withdrawn. Odds ratios are those of the cited papers and are not estimated here. None of these formulae was computed on an empirical maternal cohort, and none is validated as a risk predictor.

Results

Locked four-cohort meta-analysis: a null in adult postmortem brain

Of 468 panel genes, 392 were meta-analyzable in at least two of the four locked cohorts (208 in four, 145 in three, 39 in two). One gene, MAFK, reached FDR < 0.05 (pooled log2FC − 0.34, k = 3, I^2 0%, FDR 0.025), nominally significant in one cohort only; no gene met the high-confidence rule (Table 2; Fig. 1). A two-cohort sensitivity analysis of GSE102741 (DLPFC) and GSE28521 (cerebellum) (130 meta-analyzable genes; described in the earlier version of this paper as cortex-only) was also null, with no gene at FDR < 0.05.

The iron/redox–NRF2 genes that are higher in PD brain in this series (27) are not convergent in ASD. HMOX1 (pooled log2FC + 0.10, I^2 94%), NQO1 (− 0.01, I^2 91%), and MT2A (+ 0.26, I^2 91%) are near zero with high between-cohort heterogeneity, and their 95% confidence intervals span zero (Table 2, Fig. 1). The pooled estimates are on the same log2 fold-change scale as the companion meta-analyses, so the contrast is direct. Two of the four cohorts are cerebellum (GSE28521, GSE269105) and two are cortex (GSE102741, DLPFC; GSE64018, temporal cortex); tissue is modeled through random effects and is a heterogeneity source. A true cortex-only analysis (GSE102741 + GSE64018) was not part of the locked run.

Table 2
Random-effects (DerSimonian–Laird) pooled log2 fold-change for selected panel genes across the four locked ASD postmortem-brain cohorts.

Gene	k	Pooled log2FC	95% CI	I^2	Direction concordance	Cohorts p < 0.05	BH-FDR
MAFK	3	-0.34	-0.50 to -0.17	0%	67%	1	0.025
HMOX1	3	+ 0.10	-2.31 to + 2.51	94%	33%	2	0.99
NQO1	4	-0.01	-0.90 to + 0.89	91%	25%	2	1.00
MT2A	4	+ 0.26	-0.90 to + 1.41	91%	75%	2	0.99
FTL	4	-0.11	-0.66 to + 0.44	89%	50%	2	0.99
APOE	4	+ 0.03	-0.43 to + 0.48	74%	50%	2	0.99
AQP1	3	-0.26	-1.45 to + 0.94	71%	33%	1	0.99
NFE2L2	4	-0.05	-0.30 to + 0.21	59%	50%	1	0.99
GSS	4	-0.01	-0.24 to + 0.21	65%	75%	2	0.99
CYP26A1	2	+ 0.21	-0.32 to + 0.75	58%	50%	0	0.99
CYP26B1	4	-0.11	-0.40 to + 0.17	9%	50%	0	0.99
CYP2E1	4	-0.14	-0.47 to + 0.19	64%	75%	1	0.99

Values are those of the locked workbook. MAFK is the only panel gene at FDR < 0.05; no gene is high-confidence. Other genes were chosen to illustrate the iron/redox–NRF2, glutathione, and CYP26 axes. 95% CI = pooled ± 1.96 × SE, with SE recovered as |pooled| / z(p). Direction concordance and cohort counts use the normal-approximation cohort p value of the locked rule. Positive log2FC = higher in ASD.

Gestational-compartment tests

In maternal blood from pregnancies later resulting in ASD versus typical development (GSE148450, MARBLES (59); 56 ASD, 103 typically developing), none of 426 measured panel genes reached FDR < 0.05 within the panel. Fifteen were nominally significant (p < 0.05), fewer than the approximately 21 expected by chance, and the largest absolute change was 0.34 log2 units (BACH1). Genome-wide, no gene reached FDR < 0.05 (smallest adjusted p = 0.58). A blood transcriptome is not expected to report a germline or placental liability, so this null does not bear on the maternal-genotype hypothesis. In umbilical cord blood (GSE123302, MARBLES and EARLI (58)) the panel

was likewise null at FDR; the only two nominally lower panel genes were CYP1A1 and MAFF. Nominal single-gene calls in a null screen are not interpreted further.

Per-dataset panel dysregulation across 14 supporting datasets

Across the 14 supporting datasets, 297 of 468 panel genes were called in at least one comparison (Table 3). GSE64018 and GSE102741 in that tier are the same accessions as two locked meta-analysis cohorts and are not an independent replication of the adult-brain null. That union count describes dataset breadth; it is not an ASD signature and is not the ASD result. Per-dataset results are in Table 4.

Table 3
Descriptive per-dataset hit counts by functional hub across 14 supporting datasets (not the adult-brain meta-analysis).

Hub	Function	Genes in panel	Genes hit in ≥ 1 dataset
1	Xenobiotic & morphogen metabolism	230	136
2	Heavy-metal homeostasis	49	33
3	Neuro-vascular integrity	40	29
4	Antioxidant defense & redox homeostasis	92	66
5	Transcriptional regulation	57	33
	Total	468	297

Union count across mixed accessions; a breadth statistic only. The locked adult-brain result is 0 high-confidence genes.

Table 4
Per-dataset panel results across 14 supporting datasets (developing-brain models, first 12 rows; adult postmortem brain, last 2 rows).

Dataset	Tissue / model	n ASD/CTL	Meas.	DEGs	↑	↓	Hit % panel	Hit % meas.	Key signals
GSE187006	iPSC forebrain organoid (VPA)	—	372	86	56	30	18.4%	23.1%	SLC30A3↑(+2.95); CYP26C1↑(+2.87); UGT3A2↑(+2.66)
GSE229834	NPC/organoid (ASD)	—	373	96	81	15	20.5%	25.7%	UGT2B11↑(+6.20); GSTA2↑(+5.62); TF↑(+5.48)
GSE221923	Neural organoid (CTNNB1)	—	388	150	102	48	32.1%	38.7%	AKR1B10↑(+8.68); MT1E↑(+8.39); CES1↓(−7.26)
GSE222509	iPSC neurons (VPA)	—	365	126	92	34	26.9%	34.5%	SLC22A3↑(+8.66); GSTA1↑(+8.55); CYP1A1↑(+8.24)
GSE144736	iPSC-NPC (16p11.2 del)	—	370	67	55	12	14.3%	18.1%	CYP26C1↑(+5.58); CYP26A1↑(+3.62); ABCG2↑(+3.56)
GSE135131	iPSC/iNs (15q13.3 del)	—	342	4	2	2	0.9%	1.2%	SLC39A4↑(+1.15); CYP26A1↓(−1.03); SULT1C4↑(+0.74)
GSE210959	iPSC organoid (SHANK)	—	370	1	0	1	0.2%	0.3%	ABCA1↓(−1.30)
GSE211878	iPSC neurons (SHANK3)	—	377	20	16	4	4.3%	5.3%	CAT↓(−10.80); ICAM1↑(+2.62); CYP1B1↑(+2.22)
GSE122550	iPSC neurons (SHANK2)	—	329	14	7	7	3.0%	4.3%	CAT↑(+10.70); ICAM1↑(+3.36); CYP26C1↓(−2.95)

Dataset	Tissue / model	n ASD/CTL	Meas.	DEGs	↑	↓	Hit % panel	Hit % meas.	Key signals
GSE214323	iPSC-NPC (PTEN I135L/WT)	—	334	104	56	48	22.2%	31.1%	ABCB1↓(−7.77); CYP26A1↑(+6.82); CES1↓(−5.87)
GSE178687	DPSC neurons (PWS-ASD)	—	320	12	3	9	2.6%	3.8%	CDH5↑(+7.59); VWF↑(+3.47); CLDN11↑(+2.35)
GSE133615	iPSC neurons (16p11.2)	—	342	11	6	5	2.4%	3.2%	AKR7A3↑(+1.65); SULT1A3↑(+1.36); CYP2D6↑(+1.15)
GSE64018	Postmortem temporal cortex	12/12	406	28	27	1	6.0%	6.9%	HSPA1A↑(+3.01); HMOX1↑(+2.52); MAFF↑(+2.29)
GSE102741	Postmortem DLPFC	13/39	390	0	0	0	0.0%	0.0%	—

Threshold: BH-adjusted P < 0.05 (correction across all genes tested) and |log2FC| ≥ 0.5. Hit % panel = DEGs/468; Hit % meas. = DEGs/measurable panel genes. GSE229834: best adjusted P per gene across multiple NPC/organoid sub-comparisons. Per-dataset values are descriptive; the locked adult-brain meta-analysis is the primary result. Sources: GSE135131, Zhang et al. (18); GSE133615, Ward et al. (19); GSE178687, Victor et al. (22); GSE211878, Loureiro et al. (7); GSE64018, Gupta et al. (21).

Developing-brain tier

Across the 12 developing-brain model datasets, dataset-level measurable-basis DDI (Table 4) ranged from 0.3% in a synaptic-scaffold organoid (GSE210959) to 38.7% in an ASD organoid model (GSE221923), and individual sub-comparisons reached 51.9% (KDM2A knockdown organoids; Table 6), with the highest values in perturbations of broad regulatory or metabolic machinery (KDM2A, PTEN, valproate, CTNNB1) and near-null values in synaptic-scaffold and microdeletion models. The largest developing-brain dataset, GSE229834 (373 measurable panel genes, 96 significant), is broken down by hub in Table 5. Hub 1 shows predominantly Phase II upregulation (UGT2B11 + 6.20, GSTA2 + 5.62, GSTA1 + 5.13, CYP2W1 + 4.59). Hub 2 shows near-uniform iron and metallothionein induction (TF + 5.48, MT1H + 4.01, MT1E + 3.62, SLC40A1 + 3.43). Hub 3 is bidirectional (AQP1 and CLDN11 up; VWF and NOTCH1 down). Hub 4 is led by PON1 induction (+ 4.72), with PTGES and GGT1 up. Hub 5 shows innate-immune activation (STING1 + 2.60) against stress-response downregulation (DDIT3, HSPA1A, PPARGC1A).

Table 5
Functional hub breakdown for GSE229834 (ASD vs control; 96 significant panel genes).

Hub	Functional category	DEGs	↑	↓	Representative panel genes (log2FC)
1	Xenobiotic & morphogen metabolism	41	37	4	UGT2B11↑(+ 6.20); GSTA2↑(+ 5.62); GSTA1↑(+ 5.13); CYP2W1↑(+ 4.59)
2	Heavy-metal homeostasis	14	14	0	TF↑(+ 5.48); MT1H↑(+ 4.01); MT1E↑(+ 3.62); SLC40A1↑(+ 3.43)
3	Neuro-vascular integrity	6	4	2	AQP1↑(+ 3.03); CLDN11↑(+ 1.41); VWF↓(− 1.39); NOTCH1↓(− 1.01)
4	Antioxidant defense & redox	22	21	1	PON1↑(+ 4.72); PTGES↑(+ 2.68); GGT1↑(+ 2.23); LOXL4↑(+ 1.88)
5	Transcriptional regulation	13	5	8	STING1↑(+ 2.60); DDIT3↓(− 1.45); HSPA1A↓(− 1.39); PPARGC1A↓(− 1.35)
	Total	96	81	15	

BH-adjusted $P < 0.05$ and $|\log2FC| \geq 0.5$; best adjusted P per gene shown. All 96 significant genes are hub-assigned.

The SHANK3 knockout model (GSE211878; iPSC-derived neurons) (7) showed 20 significant panel genes (5.3% measurable-basis DDI). Catalase (CAT) was strongly suppressed (− 10.80, adjusted $P = 4.4 \times 10^{-19}$) while NFE2L2 (+ 0.57), GCLM (+ 1.35), and HMOX1 (+ 1.56) were upregulated, a pattern in which the antioxidant stress response is activated but does not offset catalase loss. ICAM1 was upregulated (+ 2.62), as in several independent models (Table 7). The SHANK2 isogenic model (GSE122550; four comparisons, 8–14 significant panel genes each) was dominated by strongly upregulated CAT (+ 10.66 to + 10.74 in three comparisons) and consistent CYP26C1 downregulation (− 2.71 to − 3.90 across three comparisons). The 15q13.3 microdeletion model (GSE135131) (18) contributed three comparisons with three, zero, and one significant panel genes. The 16p11.2 model (GSE133615) (19) was essentially null for the panel, consistent with the distributed genome-wide reprogramming reported for that CNV (23). The dental-pulp stem-cell-derived neuron model (GSE178687) (22) showed 4–14 significant panel genes across three comparisons, with ALDH3A1 strongly suppressed (− 6.93 to − 6.40) in the Prader–Willi syndrome with ASD comparisons.

Adult postmortem brain: per-dataset signals

The two adult postmortem-brain datasets in the per-dataset tier show heterogeneous signals that do not survive the cross-cohort meta-analysis. GSE64018 (temporal cortex, BA41/42/22; 12/12; PyDESeq2 on deposited raw counts) yielded 28 significant panel genes, 27 of them upregulated, a stress-response and neuroinflammatory pattern (HSPA1A + 3.01, HMOX1 + 2.52, NQO1 + 1.92, ICAM1 + 2.08). GSE102741 (DLPFC; 13/39) yielded no significant panel genes; its top genome-wide differentially expressed genes were predominantly small nucleolar and small Cajal-body RNAs, suggesting cohort-specific small-RNA biology. In the VPA forebrain-organoid series (GSE187006, a developing-brain exposure model; four cortical-region comparisons), AHR (− 2.44) and ALDH1A3 (− 2.87) were downregulated in one comparison, MGMT (+ 7.54) upregulated in another, and CYP26C1 (+ 2.82) upregulated in a third, with TJP3 upregulated in three comparisons (Table 7).

Lesion-class gradient

Recomputed under the locked per-dataset definition, the model systems show a lesion-class gradient rather than a uniform effect (Table 6). Perturbations of broad gene-regulatory or metabolic hubs produce substantial panel dysregulation: PTEN (GSE214323; WT/I135L 16.2–24.4% panel / 20.2–29.5% measurable, larger in the Apex ASD background; KO/KO 27.6–30.6% / 33.8–38.2% across two donor backgrounds), KDM2A knockdown (GSE229834; 37.0% / 44.1% in neural progenitors, 46.8% / 51.9% in cerebral organoids), valproate exposure (GSE187006 23.3% / 26.6%; GSE222509 31.0% / 36.3%), and an ASD organoid model (GSE221923; 32.1% / 38.7%). A recurrent copy-number lesion spanning a signaling kinase (16p11.2, GSE144736; deletion 17.8%, duplication 13.3%) is intermediate. Synaptic-scaffold models are near null even as isogenic contrasts (SHANK2, GSE122550, 7.1%; SHANK3, GSE210959, 0.3%), as are the 15q13.3 microdeletion (GSE135131, 1.8%) and the ASD-overlay comparison within Prader–Willi uniparental disomy (GSE178687, 5.9%). Idiopathic postmortem cortex is null (GSE102741, 0.0%), against a passage/clonal-drift floor of 1.5% (GSE214323 passage control). These per-dataset values were assembled to span mechanism classes (regulatory/metabolic hub, copy number, synaptic, environmental), not selected on outcome. The pattern is consistent with the panel reporting disruption of broad metabolic-regulatory machinery rather than the autism phenotype per se.

Table 6
Panel dysregulation by lesion class (per-dataset DDI; locked per-dataset definition).

Lesion class	Model / lesion	Dataset	DDI (% panel / measurable)	Contrast type
Broad regulatory / metabolic hub	KDM2A knockdown (organoid)	GSE229834	46.8 / 51.9	isogenic KD
	KDM2A knockdown (NPC)	GSE229834	37.0 / 44.1	isogenic KD
	PTEN KO/KO (Chap)	GSE214323	30.6 / 38.2	isogenic
	PTEN KO/KO (Apex)	GSE214323	27.6 / 33.8	isogenic
	PTEN WT/I135L (Apex)	GSE214323	24.4 / 29.5	isogenic
	PTEN WT/I135L (Chap)	GSE214323	16.2 / 20.2	isogenic
Environmental (HDAC inhibitor)	Valproate vs vehicle	GSE222509	31.0 / 36.3	exposure
	Valproate vs vehicle	GSE187006	23.3 / 26.6	exposure
Model (mixed)	ASD organoid vs control	GSE221923	32.1 / 38.7	model
Copy number (signaling)	16p11.2 deletion	GSE144736	17.8	patient-line CNV
	16p11.2 duplication	GSE144736	13.3	patient-line CNV
Synaptic scaffold	SHANK2 vs corrected	GSE122550	7.1	isogenic
	SHANK3 vs control	GSE210959	0.3	model
Other CNV / ASD overlay	15q13.3 deletion	GSE135131	1.8	patient-line CNV
	PWS-UPD + ASD vs − ASD	GSE178687	5.9	within-syndrome
Idiopathic tissue	Postmortem DLPFC (ASD vs control)	GSE102741	0.0	patient tissue
Negative control	Passage drift (WT P3 vs P5)	GSE214323	1.5	control
Flagged (confounded)	Cross-donor (Apex vs Chap, both WT)	GSE214323	34.7	cross-donor

DDI, Detoxification Dysregulation Index (BH-adjusted $P < 0.05$, correction across all genes tested, and $|\log2FC| \geq 0.5$). For the KDM2A, PTEN, valproate, and ASD-organoid rows, DDI is given on both bases, recomputed from NCBI raw counts with DESeq2; other rows give the measurable basis. “Isogenic” denotes mutant vs gene-corrected (or knockdown vs scrambled) in the same line. The cross-donor row is flagged as confounded by inter-individual variation. Values are descriptive.

Cross-dataset directional concordance

Table 7 lists panel genes significant in three or more of the 14 datasets. The most reproducible is the myelin tight-junction gene CLDN11, up in five of the six datasets in which it is significant (83%) across NPC, organoid, iPSC-neuron, and PTEN-mutant models. TJP3 is up in all five datasets in which it is significant, and CYP27A1 and EPHX1 are each up in four of five (80%). Convergence on barrier/tight-junction and oxysterol-handling genes across independent model systems is the most reproducible signal in the developing-brain tier.

Table 7
Cross-dataset directional concordance: panel genes significant in ≥ 3 comparisons.

Gene	Hub	N	Direction	Concordance	Comparisons
CLDN11	3	6	↑	83%	GSE229834↑, GSE221923↑, GSE222509↑, GSE144736↑, GSE214323↓, GSE178687↑
TJP3	3	5	↑	100%	GSE187006↑, GSE221923↑, GSE222509↑, GSE144736↑, GSE64018↑
ICAM1	3	5	↑	80%	GSE221923↓, GSE222509↑, GSE211878↑, GSE122550↑, GSE64018↑
CYP27A1	1	5	↑	80%	GSE187006↓, GSE221923↑, GSE144736↑, GSE211878↑, GSE214323↑
EPHX1	1	5	↑	80%	GSE229834↑, GSE221923↑, GSE222509↑, GSE144736↑, GSE178687↓
CAT	4	5	↓	60%	GSE221923↓, GSE211878↓, GSE122550↑, GSE214323↑, GSE178687↓
ABCB1	1	5	↓	60%	GSE187006↑, GSE222509↑, GSE144736↓, GSE122550↓, GSE214323↓
HMOX1	4	4	↑	100%	GSE187006↑, GSE222509↑, GSE211878↑, GSE64018↑
SLC2A1	3	4	↓	75%	GSE221923↓, GSE222509↓, GSE122550↑, GSE214323↓
ALDH1A3	1	4	↑	75%	GSE187006↓, GSE221923↑, GSE222509↑, GSE214323↑
CYP26B1	1	4	↑	75%	GSE187006↑, GSE221923↓, GSE222509↑, GSE214323↑
CYP26C1	1	4	Mixed	50%	GSE187006↑, GSE221923↓, GSE144736↑, GSE122550↓
CDH2	3	3	↓	67%	GSE221923↓, GSE135131↓, GSE122550↑
TP53	5	3	↓	67%	GSE187006↓, GSE222509↓, GSE64018↑
CGN	3	3	↑	67%	GSE187006↑, GSE221923↓, GSE222509↑

Genes reaching adjusted $P < 0.05$ and $|\log2FC| \geq 0.5$ in three or more primary RNA-seq comparisons. CAT is upregulated in the SHANK2 comparison (GSE122550) and in PTEN neural progenitors (GSE214323), and downregulated in SHANK3-KO neurons (GSE211878) and two other developing-brain comparisons (GSE221923, GSE178687).

CYP26 and NOS2

CYP26A1, CYP26B1, and CYP26C1, the principal Phase I metabolizers of retinoic acid, were dysregulated in five, four, and four of the 14 datasets. Direction is model-dependent: CYP26C1 is strongly downregulated in the CTNNB1 organoid (GSE221923, − 5.48) and the SHANK2 model (GSE122550, − 2.95) but upregulated in the valproate-exposed forebrain organoid (GSE187006, + 2.87) and 16p11.2-deletion progenitors (GSE144736, + 5.58), consistent with stage- and lesion-dependent retinoic-acid biology. The CYP26 axis is recurrently perturbed in ASD developing-brain models but is not significant in the adult-brain meta-analysis (CYP26A1 + 0.21, k = 2; CYP26B1 − 0.11; Table 2); in the adult analyses of this series, CYP26A1 is lower and high-confidence in AD brain (− 0.31) and MS white matter (− 0.41) and neutral in PD and ALS (11, 26, 27). NOS2 was upregulated in GSE144736 (log2FC + 2.93, adjusted $P = 3.3 \times 10^{-5}$), an undifferentiated iPSC context. In the hypothesis-generating 64-comparison GEO2R screen, including committed neural progenitors, NOS2 was lower in 95% of 20 informative comparisons, the opposite direction from the NOS2/iNOS induction reported in PD substantia nigra (27).

Maternal-axis genetic vulnerability index (research formula)

No proband detoxification-related variant in the assembled inventory reaches OR ≥ 1.5 in the ASD GWAS summaries used (10). For that reason, and because the hypothesized risk window opens before there is fetal tissue, the genetic-vulnerability formula of this series is situated in the maternal genome for ASD. Compiling the inventory required establishing, for each published association, whose genotype was measured and which outcome was reported (Table 8). That check narrows the maternal-genotype ASD evidence sharply. Of the entries previously carried as primary maternal-axis variants, the MTHFR C677T TT estimate of 1.90 (1.27–2.84) is a child genotype with no maternal subgroup (28, 30); the MTR A2756G and MTRR A66G × MTHFR TT entries do not appear in the cited CHARGE record and were misattributed, the 7.2 (2.3–22.4) figure being a child COMT 472 AA × no-prenatal-vitamins estimate (31); the MTHFR A1298C additive claim is unsupported, the cited meta-analysis reporting no association (39); the PON1 entries come from cohorts whose outcomes were Bayley, K-CPT, and WISC measures rather than ASD (15, 16, 17), with the − 108 variant not significant in trio transmission analysis (40); the GST entries are child genotypes, a medication interaction, a case-only severity analysis, and a GSTT1 × blood-manganese interaction (32, 33, 34, 35, 36, 37); and the ALDH2 figure of 5.82 (1.84–18.38) is maternal continued drinking versus non-drinking for delayed communication on the J-ASQ-3 at three years, not ASD and not a gene–environment odds ratio (38). What remains are two maternal-genotype ASD findings, both from the same CHARGE analysis (31) and both conditional on absent periconceptional prenatal vitamin use: maternal MTHFR 677 TT, OR 4.5 (1.4–14.6), and maternal CBS rs234715 GT + TT, OR 2.6 (1.2–5.4). mGVI is defined on those two. The two terms come from one analysis, are not independent, and have not been replicated as a pair. This definition is literature context, not a result of the locked analysis. The index rests on one cohort analysis and on a conditional exposure stratum; it should be read as a research formula with two literature inputs, not as a validated aggregate. The remaining inventory entries are retained in Table 8 as published context for the four axes and are excluded from the sum. Because the two inputs are fixed maternal germline variants with published exposure-conditional odds ratios, mGVI could be computed from existing maternal genotypes and tested against paired maternal-genotype and offspring-outcome cohorts (CHARGE, CHAMACOS, MARBLES, ECHO) without new enrollment, and such a test would be the first evaluation of whether it tracks risk at all.

Table 8

Literature inventory, not a result of the locked analysis. Published detoxification-gene associations grouped by whose genotype was measured and which outcome was reported. The two CHARGE maternal-genotype odds ratios are inputs to the uncomputed mGVI definition only.

Variant / entry	Gene	MAF	Published estimate and the outcome actually reported	Source
Maternal-genotype ASD findings (the mGVI sum)				
MTHFR C677T TT × no periconceptional prenatal vitamins	MTHFR	0.10–0.12	OR 4.5 (1.4–14.6). Maternal genotype; ASD in offspring; conditional on absent periconceptional prenatal vitamin use.	Schmidt et al. 2011 (31)
CBS rs234715 GT + TT × no periconceptional prenatal vitamins	CBS	Not reported here	OR 2.6 (1.2–5.4). Maternal genotype; ASD in offspring; conditional on absent periconceptional prenatal vitamin use.	Schmidt et al. 2011 (31)
Child-genotype ASD findings (context; excluded from the mGVI sum)				
MTHFR C677T TT	MTHFR	0.10–0.12	OR 1.90 (1.27–2.84), TT versus CC. Child genotype; ASD. No maternal subgroup reported.	Pan et al. 2026 (28); Li et al. 2021 (30)
MTHFR A1298C	MTHFR	0.07–0.10	Not associated with ASD in meta-analysis. The additive-in-compound-heterozygotes claim carried in the earlier version of this table was unsupported and is withdrawn.	Li et al. 2020 (39)
GSTM1 null	GSTM1	~ 0.50	OR 4.73 (1.71–13.08). Child genotype; ASD.	Hegde et al. 2024 (34)
GSTT1 null	GSTT1	0.19 EUR; 0.42 EAS	OR 14.7 (4.35–49.90) in 108 ASD and 108 control children. Child genotype; ASD; imprecise.	Hegde et al. 2024 (34)
GSTM1 null × psychotropic medication	GSTM1	~ 0.50	Medication × GSTM1 interaction only; no main-effect ASD odds ratio is reported.	Mandic-Maravic et al. 2019 (32)
GSTM1 / GSTT1 and clinical severity	GSTM1, GSTT1	Not reported here	Case-only analysis of clinical characteristics and severity; no risk odds ratio.	Mandic-Maravic et al. 2021 (33)
GSTT1 null × blood manganese	GSTT1	0.19 EUR; 0.42 EAS	GSTT1-DD × blood-manganese interaction (4.33 and 4.34; 266 child pairs); not a main-effect odds ratio. The “3.0 conservative” value carried in the earlier version of this table was unsupported and is withdrawn.	Rahbar et al. 2021 (35)
GSTP1 I105V	GSTP1	~ 0.32	Null after adjustment (36); sex-specific GSTP1 × lead interaction (37). Child genotypes.	Rahbar et al. 2020 (36); Zwiya

Variant / entry	Gene	MAF	Published estimate and the outcome actually reported	Source
Maternal-genotype ASD findings (the mGVI sum)				
				et al. 2023 (37)
Findings with non-ASD outcomes (context; excluded from the mGVI sum)				
PON1 Q192R and −108C > T × organophosphate	PON1	~ 0.26 (Q192R); ~0.12 (−108)	CHAMACOS, 353 two-year-olds; outcomes Bayley MDI/PDI and maternally reported pervasive developmental disorder symptoms. Child − 108T associated with poorer MDI; dialkyl phosphate × PON1 interactions not significant. No ASD odds ratio.	Eskenazi et al. 2010 (15)
PON1 at school age	PON1	Not reported here	PON1 not related to K-CPT or WISC outcomes. Not ASD.	Eskenazi et al. 2014 (16)
PON1 × prenatal organophosphate	PON1	Not reported here	Mount Sinai cohort, n = 404; cognitive development, not ASD. Labelled “CHARGE 2011” in the earlier version of this table; that label was wrong and is corrected here.	Engel et al. 2011 (17)
PON1 − 108C > T	PON1	~ 0.12	Trio transmission analysis; Q192R transmission in the US sample only; −108 not significant. No odds ratio and no exposure data.	D’Amelio et al. 2005 (40)
ALDH2*2 E504K × periconceptional alcohol	ALDH2	~ 0.30 EAS; rare EUR	1,727 mother–child pairs; outcome J-ASQ-3 developmental delay at three years, not ASD. The aOR 5.82 (1.84–18.38) is maternal continued drinking versus non-drinkers for delayed communication — a drinking effect, not an ALDH2 gene–environment odds ratio. ALDH2 *1/*1 drinkers showed communication delay; *1/*2 drinkers delay in all five domains.	Miyake et al. 2025 (38)

Only the two maternal-genotype ASD entries contribute to the mGVI sum; the child-genotype and non-ASD-outcome entries are retained as published context and are excluded. Rows were checked against the primary records, and estimates withdrawn from the earlier version of this table are marked as such rather than deleted silently. MAF values are for European-ancestry populations unless noted (EAS, East Asian; EUR, European). Estimates are those of the cited papers and are not estimated in this study. This table does not change the adult-brain result of 0 high-confidence genes.

Arithmetic illustration (hypothetical genotype; not a case). The figures below show how the formula behaves and are not a result of this study. For a mother carrying both qualifying variants and reporting no periconceptional prenatal vitamin use — MTHFR 677 TT (OR 4.5) and CBS rs234715 GT + TT (OR 2.6): mGVI = ln(4.5) + ln(2.6) = 1.504 + 0.956 = 2.460; cumulative OR = e^2.460 = 11.70 (check: 4.5 × 2.6 = 11.70). ASD-IDRS

at DDI 50% is 2.460 + 5.0 = 7.46, and at DDI 80% is 10.46. With mGVI = 0 and DDI = 40%, ASD-IDRS = 4.0, a nonzero score for an environmental-only profile; that property is definitional only. Three cautions apply to this illustration specifically. Multiplying published odds ratios assumes independence and no interaction between the two loci, which has not been tested and is less plausible here than for unrelated genes, since MTHFR and CBS both act in one-carbon metabolism. Both inputs come from the same cohort analysis (31), **so they are not independent replications. And both are conditional on the same exposure stratum, absent periconceptional prenatal vitamin use, so the product is defined only within that stratum and has no meaning for a supplemented pregnancy. Whether any of these scores tracks risk requires validation in paired cohorts. MFS, mGVI, and ASD-IDRS were not computed on an empirical maternal dataset in this work and do not select folate, methylcobalamin, or organophosphate-avoidance interventions for any person.**

Discussion

A null adult-brain filter score does not test the intrauterine interface

The adult-brain 468-gene analysis in ASD is a null filter score. That null is informative only if the filter is supposed to be still broken in adult brain, and for ASD I do not make that assumption. Adult postmortem brain in the locked meta-analysis — dorsolateral prefrontal cortex, temporal cortex, and two cerebellar cohorts — samples a late tissue that may be compensated. In the hypothesis considered here, the window that matters for fetal neurodevelopment closes before that tissue exists.

In the locked adult-brain meta-analysis the 468-gene redox, metal, xenobiotic, and barrier panel yielded 392 measurable genes, 1 FDR-significant gene, and 0 high-confidence genes. That result, from two cortical and two cerebellar cohorts, constrains adult-brain transcriptional scarring in this architecture. It does not constrain a maternal filter, a placental barrier, or an embryonic retinoic-acid clearance failure. The Alzheimer, Parkinson, ALS, and multiple sclerosis analyses in this series ask whether a lifelong filter failure remains visible in diseased adult tissue. ASD asks whether the same architecture failed early enough to alter fetal neuro-integrity. The architecture can be shared; the compartment cannot.

Three genomes and one interface, not one expression vector

I treat ASD risk as the sum of three genomes and one environment meeting at the maternal–fetal interface. This is not chimerism. The child is one diploid genome. The mother is a second organism. The father contributes alleles only through the sperm that became half of the fetal genome. What can fail is a negotiation across trophoblast: maternal load on one side, fetal barrier and clearance on the other (Table 9).

Table 9
Contributions of the maternal, fetal, and paternal genomes to intrauterine risk, and how each is scored in this series.

Genome	Contribution to intrauterine risk	Scoring rule in this series
Maternal	Sets the pre-conception and gestational chemical load (for example CYP1B1 rs2855658 × indoor coal-combustion exposure (Wang et al., ref. 51); MTHFR 677C > T × prenatal vitamins (Schmidt et al., ref. 31); smoking-inducible CYP1A1, general pharmacology with no ASD association cited).	Maternal genotype plus exposure. Not added to a fetal-brain or adult-brain expression score.
Fetal	Builds the placenta and the embryo. Villous trophoblast is fetal diploid tissue. CYP26B1 loss of function and CYP2E1 placental methylation are fetal.	Windowed placental RNA or methylation; Mendelian retinoic-acid clearance as a separate class.
Paternal	Transmitted half of the fetal diploid genome after fertilization. Does not set the pre-conception maternal milieu.	Scored as a transmitted fetal allele. Not a paternal intrauterine filter.

The maternal genome is the only one that can act before there is a fetus. In a case-control study of 534 mothers of fetuses or newborns with neural tube defects and 534 control mothers, maternal CYP1B1 rs2855658 genotype modified the association of indoor air pollution from smoking and coal combustion with neural-tube-defect risk in the offspring (GG mothers: OR 3.0 and 8.1 for medium and high exposure) (51). Maternal MTHFR 677C > T interacts with absent periconceptional prenatal vitamins for ASD risk in CHARGE (31). In the framework used here, those would be maternal filter failures. They would not appear as differentially expressed genes in GSE64018, and they should not be forced to.

The fetal genome includes the placenta, because villous trophoblast is fetal diploid tissue. A CYP2E1 cis-meQTL associated with placental methylation in MARBLES is a fetal allele acting in a fetal organ (47). Biallelic CYP26B1 loss of function is a fetal retinoic-acid clearance failure in the embryo (50). Paternal alleles enter only after fertilization; they can fail in the fetus or in the placenta, but they cannot set the pre-conception chemical milieu. I therefore do not apply a single parental penalty.

Ontogeny of the same architecture in human placenta

To ask whether the 468 architecture is present at the interface at all, I examined first- versus third-trimester placenta RNA-seq (GSE247382; 113 first-trimester chorionic villus samples and 42 term placentas with NCBI-processed counts; DESeq2 adjusted for fetal sex) (49). This series has no ASD label. It is ontogeny, not an outcome contrast, and it is not a result of the adult-brain meta-analysis. Of the 468 locked panel genes, 459 were present in the table and 320 (70% of the 459) were expressed at mean TPM ≥ 1 in at least one window. Placental remodeling between the windows is extensive (21,962 genes at adjusted $p < 0.05$ genome-wide), and panel genes split evenly: 136 were higher in the first trimester, 135 higher at term, and 188 outside the window. Polarity is organized by family (Table 10; Supplementary Table S4).

Table 10
Gestational-window polarity of 468-architecture families in human placenta (GSE247382; descriptive, no ASD label).

468-architecture family	GSE247382 window	Use in this companion
GST family	First-trimester high (14 of 21; none term-high)	Early conjugation program. Do not apply term polarity.
Metallothioneins, SLC40A1, FXN	First-trimester high (8 of 9 metallothioneins; SLC40A1, FXN)	Early metal-handling and export program. Do not apply term polarity.
Barrier (CLDN5) and steroid module (CYP19A1, HSD17B1, STS)	Term high (CLDN5 2.5 → 37 TPM; CYP19A1 321 → 2,425 TPM)	Late endocrine-barrier state. Do not apply first-trimester polarity.
NRF2 axis (NFE2L2, KEAP1, NQO1, HMOX1, GCLC, GCLM, TXNRD1, SRXN1)	Mostly stable (5 of 8 outside the window; KEAP1, NQO1, TXNRD1 modestly higher at term)	Constitutive at the interface; not a window marker.
Cytochrome P450 genes (55)	Split (20 term-high, 12 first-trimester high, 23 outside the window)	Family-level polarity not assignable; treat gene by gene.
CYP26A1	Floor (0.7–0.8 TPM)	Mechanistic preface only. Not a placental RNA biomarker.
CYP26B1	Term-up but low (1.5 → 3.1 TPM)	Fetal Mendelian retinoic-acid clearance locus, not a bulk-TPM weight.
CYP2E1	Low (0.4–0.6 TPM)	Cite the MARBLES DMR and cis-meQTL (47); do not use placental TPM as the ASD signal.

Window = |log2 fold-change| ≥ 0.5 and adjusted $p < 0.05$ (PyDESeq2, ~ fetal sex + trimester; 113 first-trimester, 42 term samples). TPM values are window means. TPM, transcripts per million.

GST and metallothionein genes, together with SLC40A1 and FXN, are higher in the first trimester, contemporaneous with neurulation. CLDN5 and the placental steroid genes in the panel (CYP19A1, HSD17B1, STS) are higher at term. Core NRF2-axis genes, by contrast, change little across gestation (NFE2L2, HMOX1, GCLC, GCLM, and SRXN1 fall outside the window), so the NRF2 axis is better read as constitutive at the interface than as a term marker, and cytochrome P450 genes split in both directions. Averaging the two windows erases this biology, and copying adult-brain polarity onto either window would be a methods error. CYP26A1 sits below 1 TPM and is a mechanistic preface, not a placental RNA biomarker. CYP26B1 rises at term only to about 3 TPM; I retain it as a fetal rare-variant and loss-of-function class, not as a term-placenta expression weight.

Outcome-linked placental evidence cited, not absorbed

Two external placental ASD datasets sit beside the adult-brain lock and are not rewritten as 468-panel differentially expressed genes. In MARBLES, a genome-wide-significant differentially methylated region in CYP2E1 distinguished placentas of children later diagnosed with ASD; methylation there was associated with both diagnosis and the within-DMR SNP rs1536828, and IRS2 was a second genome-wide DMR whose methylation was associated with preconceptional prenatal-vitamin use (47). In ELGAN preterm placenta (368

children; 28 with ASD at age 10), 111 genes had placental expression associated with ASD; EWSR1 and BAZ2A expression predicted case status, LRRFIP1 was under both CpG-methylation and miRNA control, and the emphasis was chromatin and immune regulation rather than CYP26 (48). GEO does not release the ASD labels with GSE154829, and I did not construct a case-control contrast from those counts.

Panel findings in developmental models

Three per-dataset findings deserve emphasis. First, the most consistent per-dataset panel signal is convergence on barrier and tight-junction genes: CLDN11 (83% concordance across six datasets), TJP3 (100% across five), and CYP27A1 and EPHX1 (80% each). Second, direction depends on tissue context: CAT is strongly upregulated in the SHANK2 isogenic model and strongly downregulated in SHANK3 knockout, and CYP26C1 changes direction between broad-regulatory and microdeletion models. Pooled hit rates obscure both. Third, the magnitude of panel dysregulation tracks the breadth of the upstream lesion rather than the ASD label: lesions in broad regulators and metabolic machinery (KDM2A, PTEN, valproate, CTNNB1) produce substantial dysregulation (roughly 20–52% on the measurable basis), synaptic-scaffold models are near null, and idiopathic postmortem cortex is null. Panel hit rate in these contrasts tracks the breadth of the engineered lesion, not the ASD label. It is not evidence that the 468-gene panel is a convergent downstream state of idiopathic autism.

Relation to the rare-variant architecture

A maternal-axis hypothesis would operate alongside, not instead of, the rare de novo and CNV architecture that explains 25–35% of ASD (4–9). High-penetrance anchors include CHD8 de novo protein-truncating variants (6), SHANK3 protein-truncating variants (7), SCN2A loss of function, and SYNGAP1 haploinsufficiency (4). Recurrent CNVs include 16p11.2 deletion, 15q11–q13 maternal duplication, and 22q11.2 deletion (8, 23, 44). Parent-of-origin of a de novo copy-number variant, including the report that 92.3% of ASD-associated 16p11.2 deletions in Fu et al. were maternal in origin (8), is not a maternal detoxification genotype and is not scored with MTHFR, PON1, or the GST nulls. In the 65–75% of cases without a high-confidence rare-variant etiology, the maternal-axis hypothesis is one testable framework among others. Priority research includes applying mGVI to existing paired maternal-genotype and offspring-outcome data in CHARGE, CHAMACOS, MARBLES, and ECHO (no new enrollment required) and a gene–environment interaction map using the full inventory in ECHO. An intervention study would follow only if those analyses support the formula.

Mechanistic hypotheses

The per-dataset and literature findings can be organized into four mechanistic categories. These are hypotheses for experimental testing, not conclusions of this paper.

Pathological failure. CYP26 downregulation in committed neural progenitors could impair retinoic-acid clearance when rhombomere specification requires sharp retinoic-acid gradients (gestation weeks 4–10). Maternal one-carbon and transsulfuration failure (MTHFR 677 TT, CBS rs234715) could limit S-adenosylmethionine supply during the epigenetic programming window (weeks 6–16); the MTR and MTRR entries that previously appeared here are not supported by the records cited for them and are withdrawn. NOS2 suppression in committed neural progenitors (discovery screen only) could impair nitric-oxide-dependent synaptic plasticity.

Compensation. GSTA1/GSTA2 induction in NPC/organoid (GSE229834) may represent partial adaptive responses. HMOX1 and NQO1 upregulation in temporal cortex (GSE64018) (21) is compatible with late compensatory activation, but it does not survive the four-cohort meta-analysis.

Inadequate adaptation. CAT suppression in SHANK3-KO iPSC neurons (− 10.80) despite NFE2L2, GCLM, and HMOX1 upregulation is compatible with an antioxidant response that does not offset catalase loss.

Maladaptive response. CYP26 failure could lead to supra-threshold retinoic acid, premature neuronal differentiation, and progenitor-pool depletion. ALDH2*2 in East Asian populations produces acetaldehyde adducts and could both deliver a teratogen and disrupt retinaldehyde-to-retinoic-acid synthesis (38). CAT overexpression in SHANK2 iPSC neurons (GSE122550, + 10.7) may perturb physiological H2O2-mediated signaling (24, 25); this requires direct experimental validation.

Cross-disease lifespan positioning

ASD is developmentally timed relative to the adult neurodegenerative companions (gestation weeks 4–28 in the maternal-axis hypothesis; PD typically midlife; AD later life) (11, 12, 26, 27). That chronology is descriptive and does not establish a single lifespan mechanism. Four cross-disease contrasts are relevant. First, NOS2/iNOS is induced in PD substantia nigra (27) but lower in ASD neural progenitors in the discovery screen. Second, CYP26 perturbation in either direction is recurrent in ASD developing-brain models, whereas in the adult analyses CYP26A1 is modestly lower in AD brain and MS white matter (log2 fold-change − 0.31 and − 0.41) and neutral in PD and ALS (11, 26). Third, a stress-response pattern (HMOX1, NQO1, HSPA1A, ICAM1 higher) appears in one ASD postmortem cohort (GSE64018) and in PD and AD postmortem tissue, although in ASD it does not survive meta-analysis. Fourth, ASD is the only disease in the series whose hypothesized risk architecture centers on the maternal–fetal interface rather than on proband-autonomous tissue pathology.

A latent, lifelong detoxification liability

The adult-brain null does not imply that autistic individuals are free of detoxification-gene liability. Under the maternal-milieu model, the autism phenotype would be driven principally by the gestational environment during the fetal window, while the offspring inherits a partial load of detoxification-gene variants from both parents that is insufficient, alone, to sustain measurable panel-wide dysregulation in the young-to-middle-aged cortex analyzed here. The model predicts that this residual liability could unmask later in life, as aging-dependent toxic burden accumulates, as the detoxification-dependent neurodegenerative diseases characterized in the companion papers. Registry epidemiology is consistent with that prediction: a Swedish national analysis of more than 2.2 million individuals found Parkinson disease 4.4-fold more common in autistic adults, predominantly before age 50 (45), and a US Medicaid study of over 1.2 million adults found early-onset dementia about 2.6-fold more prevalent in autistic adults (46). These associations have many possible explanations, including medication exposure and diagnostic ascertainment, and they do not test the detoxification hypothesis directly. On this reading the adult detoxification null is a pre-symptomatic, latent state rather than an absence of detoxification involvement, and ASD becomes a natural prospective cohort for the developmental-origins-of-neurodegeneration question that links this series.

Research questions raised by the maternal-axis literature (not clinical recommendations)

Published associations generate research questions for existing paired cohorts; they are not actionable clinical interventions derived from this paper. In CHARGE, periconceptional folic acid intake of at least 600 µg/day was

associated with lower offspring ASD odds (aOR 0.62, 95% CI 0.42–0.92; P for trend 0.001), with the strongest associations in mothers and children carrying MTHFR 677 C > T variants (29), and Surén et al. reported a 39% lower ASD risk with periconceptional folic acid in more than 85,000 mothers (OR 0.61, 95% CI 0.41–0.90) (41); prenatal vitamin use was also associated with lower recurrence in younger siblings (42). An earlier version of this paper stated that supplementation moved the odds ratio for MTHFR TT mothers from 4.5 to approximately 1.0–1.2; that figure is not in the cited record and is withdrawn. Whether downstream one-carbon or transsulfuration support modifies risk in maternal CBS rs234715 carriers is untested in humans; choline supplementation ameliorated autistic-like phenotypes in an Mthfr-deficient mouse model (14). For PON1 Q192R, the published associations depend on organophosphate exposure and were measured against cognitive rather than ASD outcomes (15–17, 40), so exposure is the modifiable variable to study and the ASD question is open. For GSTM1- and GSTT1-null genotypes, the ASD associations in the inventory are child genotypes (34) and the heavy-metal findings are interaction terms (35–37); whether maternal glutathione-supporting strategies alter offspring outcomes is untested (13). Sulforaphane-based NRF2 activation has been studied in randomized trials in autistic children (43); periconceptional maternal use would require dedicated safety evaluation. For ALDH2 carriers, avoidance of alcohol in pregnancy is already standard guidance, and the cited cohort reports developmental-screen outcomes rather than ASD (38). None of these questions is answered by the adult-brain null.

What this companion does not claim

This paper does not reopen the locked adult-brain count of 392 measurable genes, 1 FDR-significant gene, and 0 high-confidence genes. It does not treat GSE247382 as an ASD case-control. It does not merge the separate maternal-filter framework manuscript into these Results. It does not describe the maternal–fetal–paternal interface as chimerism. The discovery that remains locked is the adult-brain null. Under the interpretation that ASD risk is set where maternal, fetal, and paternal genomes meet at the trophoblast, that null remains informative. The quantitative intrauterine analysis belongs in the framework manuscript, not in this disease-restricted companion.

Limitations

Primary inference rests on four public adult postmortem-brain cohorts drawn from a small shared donor pool; sample sizes are small, and GSE269105 contributes a 3-versus-2 cerebellar subset. Two cohorts are cortex and two are cerebellum, and bulk tissue mixes cell types; no cortex-only meta-analysis was part of the locked run. GSE28521 contributes cerebellum only, on a microarray with limited panel coverage (216 panel genes), and its probe selection used the lowest-p probe for the 34 genes with more than one probe. The locked pipeline used a normal-approximation cohort p value and, where applicable, per-gene probe selection; in the Parkinson companion these inflated cohort-level evidence (27), which could only have added, not removed, significant calls here. Per-dataset statistics come from heterogeneous sources (author-deposited DESeq2 tables, GEO2R, and local DESeq2 or PyDESeq2) and are descriptive. The 64-comparison screen used covariate-unadjusted GEO2R and is hypothesis-generating only. GSE30573 (three ASD cases selected for marked A2BP1/FOX1 downregulation and three controls) was excluded for donor overlap and is not interpreted. The placental ontogeny analysis has no ASD label, uses NCBI-processed counts for 155 of the 167 deposited samples, and treats 18 pregnancies sampled in both trimesters as independent. The literature inventory in Table 8 is the weakest part of this paper and its limitations are specific. A source check against the primary records showed that most entries previously carried as maternal-axis variants are child genotypes, non-ASD outcomes, interaction terms rather than main effects, or misattributions; those estimates are withdrawn or relabelled, and the inventory

is correspondingly smaller than in the earlier version. After that check only two maternal-genotype ASD findings remain, both from one CHARGE analysis (31) and both conditional on absent periconceptional prenatal vitamin use, so mGVI rests on a single cohort analysis within one exposure stratum, has no independent replication, and is defined only for unsupplemented pregnancies. Its two inputs act in the same metabolic pathway, so the independence that the additive-log form assumes is unlikely to hold. Published estimates throughout the inventory come from studies of varying design and size, several small, and some are imprecise: the GSTT1 null odds ratio of 14.7 (95% CI 4.35–49.90) rests on three null genotypes among 108 controls, and an interval spanning more than a tenfold range should not be read as a point estimate (34). mGVI, ASD-IDRS, and MFS are uncalibrated and were not computed on any maternal cohort. None of this bears on the adult-brain result, which does not depend on the inventory.

Declarations

Ethics approval

The analyses used only publicly available, de-identified gene-expression data from the NCBI Gene Expression Omnibus. Those datasets carry the ethical oversight of their originating studies. No identifiable private information was accessed, and no human subjects were enrolled, recruited, or intervened upon by the author.

Consent to participate

Not applicable; no human participants were enrolled.

Consent to publish

Not applicable.

Funding

This research received no external funding and was conducted independently through Sirius Neuroscience, LLC.

Author contributions

M.E.M. is the sole author and performed all aspects of this work: conceptualization, panel application, dataset analysis, interpretation, and manuscript writing.

Acknowledgments

I acknowledge the GEO investigators who deposited the transcriptomic datasets analyzed here, including the Voineagu et al. (20), Gupta et al. (21), Victor et al. (22), Zhang et al. (18), Ward et al. (19), and Gonzalez et al. (49) study teams, and the CHARGE, CHAMACOS, MARBLES, ELGAN, and ECHO investigators whose work grounds the maternal-axis inventory and the placental context.

Competing interests

The author is the sole inventor on a filed patent application relating to panel-based research scoring methods that use the locked 468-gene list. MFS, mGVI, and ASD-IDRS in this paper are unvalidated and were not computed on empirical maternal samples. The application did not determine gene membership, the high-confidence rule, or the reported results. The author declares no other competing interests.

Data availability

Locked adult-brain accessions are GSE102741, GSE28521, GSE269105, and GSE64018. Other GEO accessions are supporting developmental, model, gestational-compartment, or placental-ontogeny datasets (Supplementary Table S1). The locked 468-gene panel, excluded-symbol list, pipeline, and locked per-disease meta counts are deposited at Zenodo version 1.0 (https://doi.org/10.5281/zenodo.22178094); version 1.1 (https://doi.org/10.5281/zenodo.22181129) adds the per-gene meta-analysis tables, including the ASD table. The all-versions DOI https://doi.org/10.5281/zenodo.22178093 resolves to the latest version. Supplementary Table S4 (GSE247382 placental ontogeny, every panel gene) is a separate workbook (McCaulley_ASD_Supplementary_Table_S4_GSE247382_placental_ontogeny_2026-10-14.xlsx).

References

1. American Psychiatric Association (2022) Diagnostic and Statistical Manual of Mental Disorders. Text Revision (DSM-5-TR), 5th edn. American Psychiatric Publishing
2. Maenner MJ et al (2025) Prevalence and early identification of autism spectrum disorder among children aged 4 and 8 years — Autism and Developmental Disabilities Monitoring Network, 16 sites, United States, 2022. MMWR Surveill Summ 74:1–22. https://doi.org/10.15585/mmwr.ss7402a1
3. Lavelle TA et al (2014) Economic burden of childhood autism spectrum disorders. Pediatrics 133:e520–e529. https://doi.org/10.1542/peds.2013-0763
4. Satterstrom FK et al (2020) Large-scale exome sequencing study implicates both developmental and functional changes in the neurobiology of autism. Cell 180:568–584. https://doi.org/10.1016/j.cell.2019.12.036
5. Qiu S et al (2022) Genetics of autism spectrum disorder: an umbrella review of systematic reviews and meta-analyses. Transl Psychiatry 12:249. https://doi.org/10.1038/s41398-022-02009-6
6. Bernier R et al (2014) Disruptive CHD8 mutations define a subtype of autism early in development. Cell 158:263–276. https://doi.org/10.1016/j.cell.2014.06.017
7. Loureiro LO et al (2021) A recurrent SHANK3 frameshift variant in autism spectrum disorder. npj Genom Med 6:91. https://doi.org/10.1038/s41525-021-00254-0
8. Fu JM, Satterstrom FK et al (2022) Rare coding variation provides insight into the genetic architecture and phenotypic context of autism. Nat Genet 54:1320–1331. https://doi.org/10.1038/s41588-022-01104-0
9. Zhou X et al (2022) Integrating de novo and inherited variants in 42,607 autism cases identifies mutations in new moderate-risk genes. Nat Genet 54:1305–1319. https://doi.org/10.1038/s41588-022-01148-2
10. Grove J et al (2019) Identification of common genetic risk variants for autism spectrum disorder. Nat Genet 51:431–444. https://doi.org/10.1038/s41588-019-0344-8

11. McCaulley ME (2026) Transcriptomic associations of a pre-specified 468-gene redox and xenobiotic-metabolism panel across five neurological disorders, with a published-variant inventory. Methods-and-panel manuscript of this series, under peer Rev Mol Neurobiol
12. McCaulley ME (2026) Impaired pathways of detoxification and risk of Alzheimer's disease: differential gene expression studies via gene set expression analysis. J Alzheimers Dis Rep 10:25424823261419382. https://doi.org/10.1177/25424823261419382
13. James SJ et al (2006) Metabolic endophenotype and related genotypes are associated with oxidative stress in children with autism. Am J Med Genet B 141B:947–956. https://doi.org/10.1002/ajmg.b.30366
14. Vainer E et al (2020) The influence of choline treatment on behavioral and neurochemical autistic-like phenotype in Mthfr-deficient mice. Transl Psychiatry 10:307. https://doi.org/10.1038/s41398-020-01002-1
15. Eskenazi B et al (2010) PON1 and neurodevelopment in children from the CHAMACOS study exposed to organophosphate pesticides in utero. Environ Health Perspect 118:1775–1781. https://doi.org/10.1289/ehp.1002234
16. Eskenazi B et al (2014) Organophosphate pesticide exposure, PON1, and neurodevelopment in school-age children from the CHAMACOS study. Environ Res 134:149–157. https://doi.org/10.1016/j.envres.2014.07.001
17. Engel SM et al (2011) Prenatal exposure to organophosphates, paraoxonase 1, and cognitive development in childhood. Environ Health Perspect 119:1182–1188. https://doi.org/10.1289/ehp.1003183
18. Zhang S et al (2021) Network effects of the 15q13.3 microdeletion on the transcriptome and epigenome in human-induced neurons. Biol Psychiatry 89:497–509. https://doi.org/10.1016/j.biopsych.2020.06.021
19. Ward TR et al (2025) Cell-type specific global reprogramming of the transcriptome and epigenome in induced neurons with the 16p11.2 neuropsychiatric CNVs. Eur J Hum Genet 33:1698–1707. https://doi.org/10.1038/s41431-025-01856-3
20. Voineagu I et al (2011) Transcriptomic analysis of autistic brain reveals convergent molecular pathology. Nature 474:380–384. https://doi.org/10.1038/nature10110
21. Gupta SK et al (2014) Transcriptome analysis reveals dysregulation of innate immune response genes and neuronal activity-dependent genes in autism. Nat Commun 5:5748. https://doi.org/10.1038/ncomms6748
22. Victor AK et al (2021) Molecular changes in Prader-Willi syndrome neurons reveals clues about increased autism susceptibility. Front Mol Neurosci 14:747855. https://doi.org/10.3389/fnmol.2021.747855
23. Niarchou M et al (2019) Psychiatric disorders in children with 16p11.2 deletion and duplication. Transl Psychiatry 9:8. https://doi.org/10.1038/s41398-018-0339-8
24. Zhang H et al (2022) Oxidative stress in autism spectrum disorder — current progress of mechanisms and biomarkers. Front Psychiatry 13:813304. https://doi.org/10.3389/fpsyt.2022.813304
25. Kheder A et al (2025) Oxidative markers and SOD variant: predictors of autism severity and susceptibility. Future Sci OA 11:2483628. https://doi.org/10.1080/20565623.2025.2483628
26. McCaulley ME (2026) A locked 468-gene detoxification panel in Alzheimer's disease brain, liver, and blood: 141 high-confidence cerebral associations including lower CYP46A1 transcript abundance, and a 12-sample hepatic CYP7A1 signal. Research Square, version 1 https://doi.org/10.21203/rs.3.rs-10999456/v1
27. McCaulley ME (2026) Panel-gene transcriptomic associations and published-variant architecture in Parkinson disease. Res Square version 1. https://doi.org/10.21203/rs.3.rs-11097203/v1

28. Pan Y, Mcdill B, Mooney M (2026) The contribution of ethnicity to the association of MTHFR variants C677T and A1298C with autism spectrum disorder: a meta-analysis. Brain Sci 16:93. https://doi.org/10.3390/brainsci16010093
29. Schmidt RJ, Tancredi DJ, Ozonoff S, Hansen RL, Hartiala J, Allayee H, Schmidt LC, Tassone F, Hertz-Picciotto I (2012) Maternal periconceptional folic acid intake and risk of autism spectrum disorders and developmental delay in the CHARGE (CHildhood Autism Risks from Genetics and Environment) case-control study. Am J Clin Nutr 96:80–89 PMID 22648721. https://doi.org/10.3945/ajcn.110.004416
30. Li CX et al (2021) Association between MTHFR C677T polymorphism and susceptibility to autism spectrum disorders: a meta-analysis in Chinese Han population. Front Pediatr 9:598805. https://doi.org/10.3389/fped.2021.598805
31. Schmidt RJ, Hansen RL, Hartiala J, Allayee H, Schmidt LC, Tancredi DJ, Tassone F, Hertz-Picciotto I (2011) Prenatal vitamins, one-carbon metabolism gene variants, and risk for autism. Epidemiology 22, 476–485 PMID 21610500. https://doi.org/10.1097/EDE.0b013e31821d0e30
32. Mandic-Maravic V et al (2019) Autism spectrum disorders and perinatal complications — is oxidative stress the connection? Front Psychiatry 10:675. https://doi.org/10.3389/fpsyt.2019.00675
33. Mandic-Maravic V et al (2021) Glutathione S-transferase polymorphisms and clinical characteristics in autism spectrum disorders. Front Psychiatry 12:672389. https://doi.org/10.3389/fpsyt.2021.672389
34. Hegde R, Hegde S, Kulkarni SS, Das KK, Gai PB (2024) Glutathione S transferase theta1 and mu1 (GSTT1 and GSTM1) deletion among autistic population of India. Curr Psychiatry Res Rev 20:152–161. https://doi.org/10.2174/2666082219666230302142608
35. Rahbar MH et al (2021) Interaction of blood manganese concentrations with GSTT1 in relation to autism spectrum disorder in Jamaican children. J Autism Dev Disord 51:1953–1965. https://doi.org/10.1007/s10803-020-04677-z
36. Rahbar MH et al (2020) Interaction between a mixture of heavy metals and GSTP1, GSTT1, and GSTM1 in relation to autism spectrum disorder. Res Autism Spectr Disord 79:101681. https://doi.org/10.1016/j.rasd.2020.101681
37. Zwiya H et al (2023) Are there sex differences in interactive associations of environmental exposure to lead, mercury, and manganese with GST genes in relation to ASD. Jamaican children? Res Autism Spectr Disord 105:102162. https://doi.org/10.1016/j.rasd.2023.102162
38. Miyake K et al (2025) Maternal alcohol consumption during pregnancy and child development: role of ADH1B and ALDH2 gene polymorphisms — The Yamanashi Adjunct Study of the Japan Environment and Children's Study. Alcohol Clin Exp Res 49:117–127. https://doi.org/10.1111/acer.15487
39. Li Y et al (2020) Association between MTHFR C677T/A1298C and susceptibility to autism spectrum disorders: a meta-analysis. BMC Pediatr 20:449. https://doi.org/10.1186/s12887-020-02330-3
40. D'Amelio M et al (2005) Paraoxonase gene variants are associated with autism in North America, but not in Italy: possible regional specificity in gene-environment interactions. Mol Psychiatry 10:1006–1016. https://doi.org/10.1038/sj.mp.4001714
41. Surén P et al (2013) Association between use of folic acid supplements and risk of autism spectrum disorders in children. JAMA 309:570–577. https://doi.org/10.1001/jama.2012.155925
42. Schmidt RJ et al (2019) Association of maternal prenatal vitamin use with risk for autism spectrum disorder recurrence in young siblings. JAMA Psychiatry 76:391–398.

https://doi.org/10.1001/jamapsychiatry.2018.3901

43. Zimmerman AW et al (2021) Randomized controlled trial of sulforaphane and metabolite discovery in children with autism spectrum disorder. Mol Autism 12:38. https://doi.org/10.1186/s13229-021-00447-5
44. Sanders SJ et al (2011) Multiple recurrent de novo CNVs, including duplications of the 7q11.23 Williams syndrome region, are strongly associated with autism. Neuron 70:863–885. https://doi.org/10.1016/j.neuron.2011.05.002
45. Yin W, Reichenberg A, Schnaider Beeri M, Levine SZ, Ludvigsson JF, Figee M, Sandin S (2025) Risk of Parkinson disease in individuals with autism spectrum disorder. JAMA Neurol 82:687–695. https://doi.org/10.1001/jamaneurol.2025.1284
46. Vivanti G, Tao S, Lyall K, Robins DL, Shea LL (2021) The prevalence and incidence of early-onset dementia among adults with autism spectrum disorder. Autism Res 14:2189–2199. https://doi.org/10.1002/aur.2590
47. Zhu Y, Mordaunt CE, Yasui DH, Marathe R, Coulson RL, Dunaway KW, Jianu JM, Walker CK, Ozonoff S, Hertz-Picciotto I, Schmidt RJ, LaSalle JM (2019) Placental DNA methylation levels at CYP2E1 and IRS2 are associated with child outcome in a prospective autism study. Hum Mol Genet 28:2659–2674. https://doi.org/10.1093/hmg/ddz084
48. Freedman AN, Clark J, Eaves LA, Roell K, Oran A, Koval L, Rager J, Santos HP Jr, Kuban K, Joseph RM, Frazier J, Marsit CJ, Burt AA, O'Shea TM, Fry RC (2023) A multi-omic approach identifies an autism spectrum disorder (ASD) regulatory complex of functional epimutations in placentas from children born preterm. Autism Res 16:918–934. https://doi.org/10.1002/aur.2915
49. Gonzalez TL, Wertheimer S, Flowers AE, Wang Y, Santiskulvong C, Clark EL, Jefferies CA, Lawrenson K, Chan JL, Joshi NV, Zhu Y, Tseng HR, Karumanchi SA, Williams J III, Pisarska MD (2024) High-throughput mRNA-seq atlas of human placenta shows vast transcriptome remodeling from first to third trimester. Biol Reprod 110:936–949. https://doi.org/10.1093/biolre/ioae007
50. Laue K, Pogoda H-M, Daniel PB, van Haeringen A, Alanay Y, von Ameln S, Rachwalski M, Morgan T, Gray MJ, Breuning MH, Sawyer GM, Sutherland-Smith AJ, Nikkels PG, Kubisch C, Bloch W, Wollnik B, Hammerschmidt M, Robertson SP (2011) Craniosynostosis and multiple skeletal anomalies in humans and zebrafish result from a defect in the localized degradation of retinoic acid. Am J Hum Genet 89:595–606. https://doi.org/10.1016/j.ajhg.2011.09.015
51. Wang L, Li Z, Jin L, Li K, Yuan Y, Fu Y, Zhang Y, Ye R, Ren A (2014) Indoor air pollution and neural tube defects: effect modification by maternal genes. Epidemiology 25:658–665. https://doi.org/10.1097/EDE.0000000000000129
52. Barrett T et al (2013) NCBI GEO: archive for functional genomics data sets—update. Nucleic Acids Res 41:D991–D995. https://doi.org/10.1093/nar/gks1193
53. DerSimonian R, Laird N (1986) Meta-analysis in clinical trials. Control Clin Trials 7:177–188. https://doi.org/10.1016/0197-2456(86)90046-2
54. Benjamini Y, Hochberg Y (1995) Controlling the false discovery rate: a practical and powerful approach to multiple testing. J R Stat Soc Ser B Stat Methodol 57:289–300. https://doi.org/10.1111/j.2517-6161.1995.tb02031.x
55. Love MI, Huber W, Anders S (2014) Moderated estimation of fold change and dispersion for RNA-seq data with DESeq2. Genome Biol 15:550. https://doi.org/10.1186/s13059-014-0550-8

56. Muzellec B, Teleńczuk M, Cabeli V, Andreux M (2023) PyDESeq2: a python package for bulk RNA-seq differential expression analysis. Bioinformatics 39:btad547. https://doi.org/10.1093/bioinformatics/btad547
57. Smyth GK (2004) Linear models and empirical Bayes methods for assessing differential expression in microarray experiments. Stat Appl Genet Mol Biol 3., Article 3 (https://doi.org/10.2202/1544-6115.1027
58. Mordaunt CE, Park BY, Bakulski KM et al (2019) A meta-analysis of two high-risk prospective cohort studies reveals autism-specific transcriptional changes to chromatin, autoimmune, and environmental response genes in umbilical cord blood. Mol Autism 10:36. https://doi.org/10.1186/s13229-019-0287-z
59. Zhu Y, Mordaunt CE, Durbin-Johnson BP, Caudill MA, Malysheva OV, Miller JW, Green R, James SJ, Melnyk SB, Fallin MD, Hertz-Picciotto I, Schmidt RJ, LaSalle JM (2021) Expression changes in epigenetic gene pathways associated with one-carbon nutritional metabolites in maternal blood from pregnancies resulting in autism and non-typical neurodevelopment. Autism Res 14:11–28. https://doi.org/10.1002/aur.2428
60. Supplementary, Tables
61. Supplementary Table S Dataset metadata: 30 RNA-seq comparisons across 18 assembled GEO accessions (the deleted GSE173687 is listed for transparency and not analyzed), plus the gestational-compartment and placental datasets

Figures

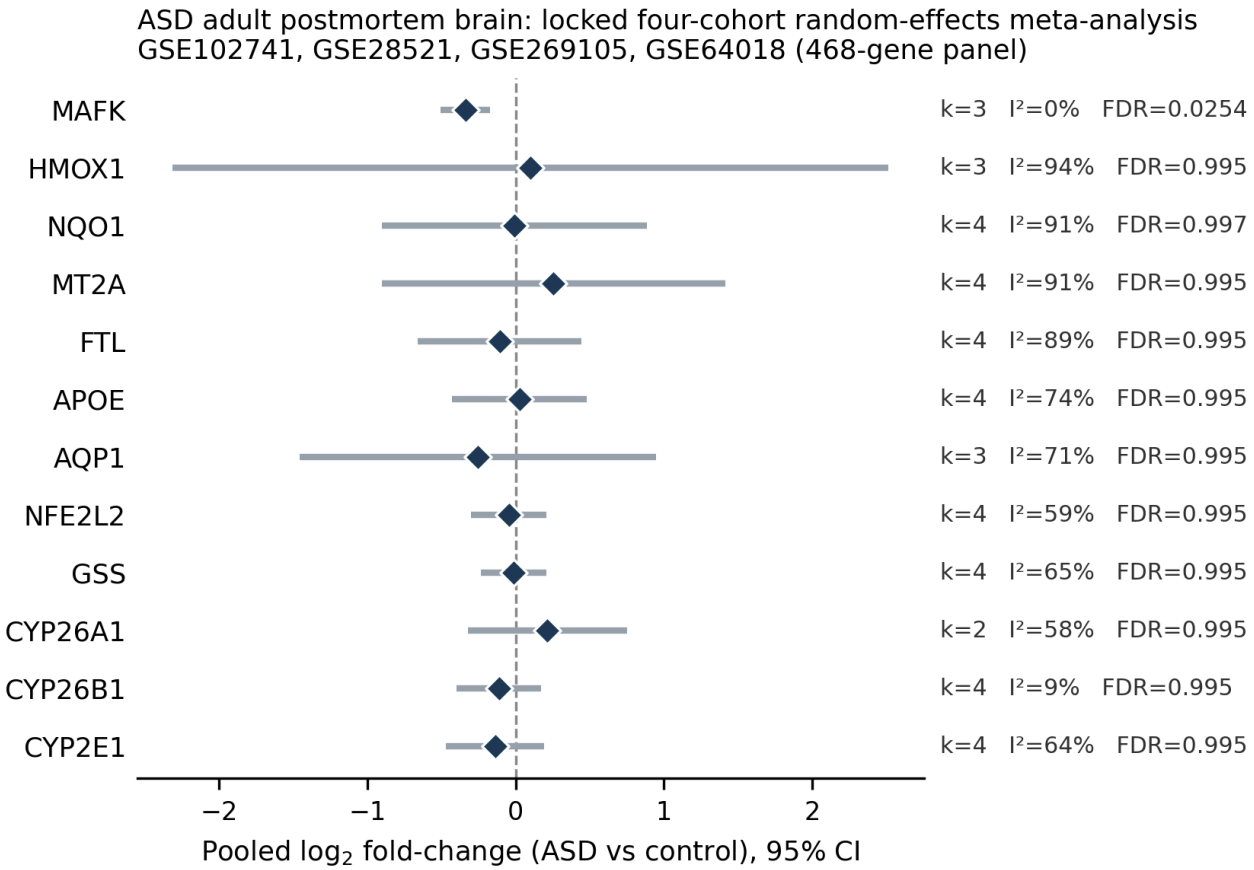


Figure 1

Fig. 1. Forest plot of the locked four-cohort ASD postmortem-brain meta-analysis (random effects, DerSimonian–Laird; GSE102741 DLPFC, GSE64018 temporal cortex, GSE28521 and GSE269105 cerebellum). Diamonds are pooled log2 fold-changes (ASD versus control) with 95% confidence intervals computed as the pooled estimate ± 1.96 × SE, with SE recovered as |pooled| / z(p); k, I^2, and BH-FDR are printed at the right. MAFK is the only panel gene at FDR < 0.05 and its interval excludes zero; every other interval crosses zero, including the iron/redox–NRF2 genes (HMOX1, NQO1, MT2A) that are higher in the neurodegenerative companions. No gene is high-confidence. Values are those of the locked workbook.

Supplementary Files

This is a list of supplementary files associated with this preprint. Click to download.

- McCaulleyASDSupplementaryTableS4GSE247382placentalontogeny20261014.xlsx